Radial Structure of Fluctuation in Electron ITB Plasmas of LHD

S. Inagaki 1,2), N. Tamura 3), T. Tokuzawa 3), K. Ida 2,3), T. Shimozuma 3), S. Kubo3), H. Tsuchiya 3), Y. Nagayama 3), K. Kawahata 3), S. Sudo 3), K. Itoh2,3), S.-I. Itoh1,2) and LHD Experimental Group

1) Research Institute for Applied Mechanics, Kyushu University, 6-1 Kasuga-Koen, Kasuga-city, 816-8580, Japan
2) Itoh Research Center for Plasma Turbulence, Kyushu University, Kasuga 816-8580, Japan
3) National Institute for Fusion Science, 322-6, Oroshi-cho, Toki-city, 509-5292, Japan

E-mail : inagaki@riam.kyushu-u.ac.jp

Abstract. Macro-scale fluctuations with long radial correlation are identified not only in the L-mode plasmas but also in plasmas with internal transport barrier (ITB) in Large Helical Device (LHD). Correlation technique has successfully realized the observation of electron temperature fluctuations, which are characterized by their correlation length comparable to plasma minor radius, with low frequency of ~1-7kHz, ballistic radial propagation (at speed of ~1km/s, order of diamagnetic drift velocity). Radial structures of fluctuations are qualitatively different between the L-mode and ITB plasmas. Dynamic response of this long-range temperature fluctuation is observed in perturbative experiments. Distortion of wave-front coincident with reduction of transport is discussed.

1. Introduction

The internal transport barrier (ITB), a steep temperature gradient that is observed in the plasma interior, has the potential to enhance performance of burning plasmas such as ITER. Thus the precise understanding is demanded and the phenomenological understanding of ITB has been in progress [1-3]. The study of ITB on Large Helical Device (LHD) [4, 5] has demonstrated that the transition in core suggested a nonlocal dynamics (analogous to the fast response of core after H-L transition [6]). Nonlocal dynamics have also been observed in L-mode plasmas [7-10]. Macro-scale fluctuations with long distance correlation and avalanche phenomena are possible candidates to explain the nonlocal nature role in transport. [11-15]. Identification of such fluctuations and illumination of their impacts on confinement are urgent problems for both tokamaks and helical plasmas.

This paper presents identification of macro-scale fluctuations both in L-mode and ITB plasmas in LHD. Observation of dynamic response of long-range fluctuations is also reported. This discovery has distinctive impact on two aspects. First, in nuclear fusion research, the fast edge-core coupling has significant impacts on plasma control. At the same time, phase dynamics in the nonlinear oscillating system is, in one hand, an academic challenge for comprehensive understanding of spatiotemporal structure of turbulence.

2. Long-Range Fluctuation in L-mode Plasmas of LHD

Recently, low frequency temperature fluctuations with long distance correlation were discovered on L-mode plasmas of Large Helical Device (LHD) [16] using global correlation measurement between fluctuations or its envelope obtained from multi-channel ECE system [17], a micro-wave reflectometer [18] and magnetic probe array [19] arranged over the full gamut of torus. The target L-mode plasma is produced with neutral beam injection of 2 MW and electron cyclotron resonant heating (ECRH) of P_{ECH}=0.8 MW is superimposed at the plasma centre. Typical parameters in this experiment are as follows: a major radius R of 3.5

m, an averaged minor radius of 0.6 m, and a magnetic field strength B_{ax} of 2.83 T on the axis, the line-averaged density $\bar{n}_e$ of 0.4×10^{19} m^{-3}, central electron temperature $T_e(0)$ of 4 keV, the volume averaged β of 0.1 % and the electron collision frequency normalized by bounce frequency of helical ripple-trapped orbit of 0.03. The heat diffusivity estimated from the power balance equation is ~ 3 m^2/s at the half of radius. Global correlation analysis is applied during the quiet period, where the plasma has no MHD activity, without a transport barrier nor power modulation. The electron temperature fluctuations ($\tilde{T}_e$) are observed with a multi-channel ECE radiometer. Figure 1(a) shows the cross-power spectrum of $\tilde{T}_e$ between two neighboring points at ρ~0.4, where ρ is the normalized radius. An unambiguous peak around a few kHz with ~ 1 kHz bandwidth is visible in spectrum. The radial profile of $\tilde{T}_e$ amplitude in the frequency range of 1.5-3.5kHz is shown in Figs. 1(b)(c), and $\tilde{T}_e$ exceeds 20 eV at ρ~0.4. Magnetic probe measures weak signal in the relevant frequency range ($\tilde{b}/B_{ax}<10^{-6}$) at probe position and thus observed $\tilde{T}_e$ are not the MHD instability such as interchange modes. The ECE signals have unambiguous cross-correlation with magnetic probe signals at f = 2.5 and 3.5 kHz. The cross-phase indicates that the toroidal mode number is n = 1.

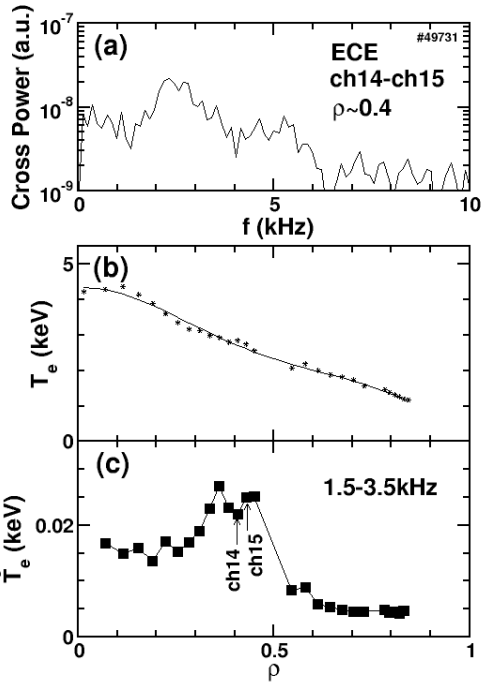

FIG. 1. (a) Typical cross-power spectrum of ECE signals. Radial profiles of (b) T_e and (c) amplitude of fluctuations in frequency band of 1.5-3.5kHz.

Spatiotemporal structure of T_e fluctuations is determined by two-point two-time correlation of $\tilde{T}_e$ in the range of 1.5-3.5 kHz (band-pass-filter is applied) at different radii. Correlation function between the ECE signals at two different points in space and time is defined as

$$c(\rho,\rho_{ref},\tau)=\frac{\langle f(\rho,t)f(\rho_{ref},t+\tau)\rangle}{\sqrt{\langle f^2(\rho,t)\rangle\langle f^2(\rho_{ref},t)\rangle}}.$$

Where τ is time lag and $f(\rho,\tau)$ is time series of the ECE channel located at ρ and $\langle\rangle$ indicates temporal averaging, defined as $\langle h(t)\rangle=\frac{1}{T}\int_0^T h(t)dt$.

Figure 2(a) shows a contour plot of correlations of $\tilde{T}_e$ (which is band-passed in the frequency range of 1.5-3.5 kHz) at 28- ECE channels with that of the reference channel at ρ_{ref}=0.43. The fluctuations have a long radial correlation, which extends from the centre to peripheral region. The radial wavelength is of the order of the plasma radius. The wave propagates from core to edge. The propagation is ballistic and not diffusive. The radial phase velocity is extremely fast around ρ~0.5 and ~ 1 km/s on radial average, which is of the order of the diamagnetic drift velocity. Poloidal structure of fluctuations $\delta T_e(\rho,\theta)$ can be reconstructed from correlation pattern taking into consideration of the form $\tilde{T}_e(\rho,\theta,t)=\delta T_e(\rho)\exp(im\theta-i\omega t)$ for which ω is given by the peak of spectrum. Here θ is poloidal angle coordinate, m is the poloidal mode number and the frequency is in the laboratory frame. In order to estimate the frequency in the plasma frame, Doppler shift due to $\boldsymbol{E}\times\boldsymbol{B}$ drift should be taken into account. The cross-phase

between the ECE signal and a poloidal magnetic probe array indicates the poloidal mode number m = 1-2. The $\tilde{T}_e$ structure on the poloidal cross section is reconstructed using the information m=1 and is shown in Fig. 2(b). Spiral structure connects core and peripheral regions.

The density fluctuations with broad spectrum (1~100kHz) are observed with a reflectometer. In order to estimate low frequency large-scale potential fluctuations that co-exist with low frequency long-range T_e fluctuations, the envelope of density fluctuations in the high frequency band is extracted [16]. High-pass-filter (>100kHz) is applied to reflectometer signal and its envelope is calculated. The Fourier spectrum of envelope shows broad peaks around 1.5kHz and 2.5kHz. Envelope of density fluctuations in the high frequency band indicates the existence of modulator of micro-scale fluctuations. Significant cross-correlation between the modulator and long-range T_e fluctuations is found in the frequency range of 0.2 to 5 kHz and the wide radial region. The bi-coherence analysis demonstrates that large-scale $\tilde{T}_e$ around 2.5 kHz couples non-linearly with microscopic density fluctuations [16].

Kubo number is much smaller than one in these experiments. The contribution of long-range fluctuation to transport in stationary state, therefore, may be evaluated by use of random walk model. An estimated effective diffusion coefficient of ~ 0.2 m^2/s in the L-mode [16] is a small portion (order of 10^{-1}) of heat diffusivity estimated from power balance equation in stationary state.

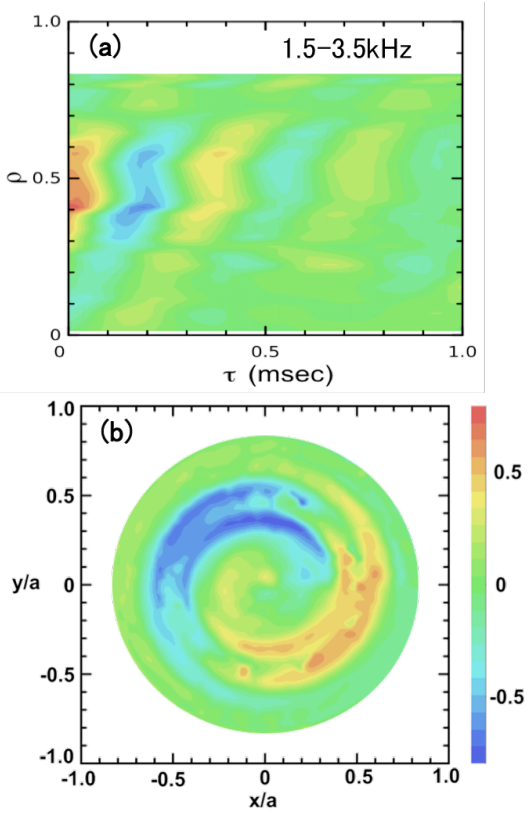

FIG. 2. (a) Contour plot of the cross-correlation function of the low frequency component (1.5-3.5 kHz) of $\tilde{T}_e$ from 28-ECE channels with that of the reference channel at ρ=0.43. (b) Reconstructed image plot of $\tilde{T}_e$ structure on the poloidal cross-section. Here a is plasma radius.

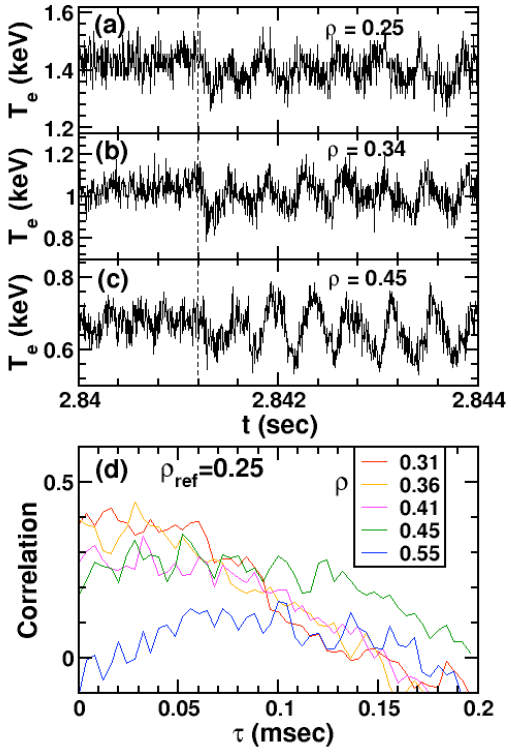

FIG. 3. (a)-(c) Time evolution of T_e at three different radii during the fluctuation burst. (d)Cross-correlation function. The reference channel is located at ρ=0.25.

Abrupt change of amplitude of the long-range fluctuations is observed and illustrated in Figs. 3(a)-(c). The change of amplitude propagates from core to edge. The cross correlation functions calculated around the onset of the amplitude burst (the time window of 2.8402-2.8418 sec) demonstrates that the time-delay exists between ρ=0.25 to 0.58 as shown in Fig. 3(d). Time scale of radial propagation is the order of the 0.1 msec in this case. This observation indicates that not only wave-front of fluctuations but also the amplitude of fluctuations (i.e., the change of effective thermal diffusivity) have ballistic radial propagation. Abrupt propagation of the order of 0.1 msec is 50-100 times faster than what would be expected from diffusive transport models. For the transient transport, therefore, this fluctuation can play a dominant role in fast transport response.

3. Long-Range Fluctuation in ITB plasmas of LHD

The e-ITB is formed with center focused electron cyclotron heating with power of P_{ECH} = 0.4-1.1MW in LHD [20]. Typical radial profiles of T_e are shown in Fig. 4(a). Here the line averaged density is 0.5×10^{19} m^{-3}. In the low heating power case (0.4 MW), narrow and weak barrier is formed. The barrier is found to be wider and stronger in the high heating power (1.1 MW) case. The T_e fluctuations in the frequency band of 2.5-4.5 kHz and 5-7 kHz are excited in low- (Fig. 4(b)) and high heating power case (Fig. 4(c)), respectively. Magnetic probe arrays detected stronger signals (compared to one in the L-mode plasma) in the relevant frequency range and suggest that $\tilde{T}_e$ at 3 kHz has n/m = 1/1 or 1/2 and one at 6 kHz has n/m = 1/2 or 1/3. Contour plots of correlations of $\tilde{T}_e$ in Figs 4(b)(c) show that the ballistic radial propagation of fluctuation at speed of 2-5 km/s, which is the order of diamagnetic drift velocity in the both cases. The radial propagation pattern is qualitatively different between the L-mode and ITB plasmas. A node is formed in the core region (ρ~0.25) in the ITB cases. Noting that $\tilde{T}_e$ is small and it is difficult to distinguish $\tilde{T}_e$ from noise in the region of ρ>0.45. The difference of radial propagation pattern of long-range fluctuation is one of the key issues to understand the ITB formation. Details of quantitative comparison will be the subjects of future experiments.

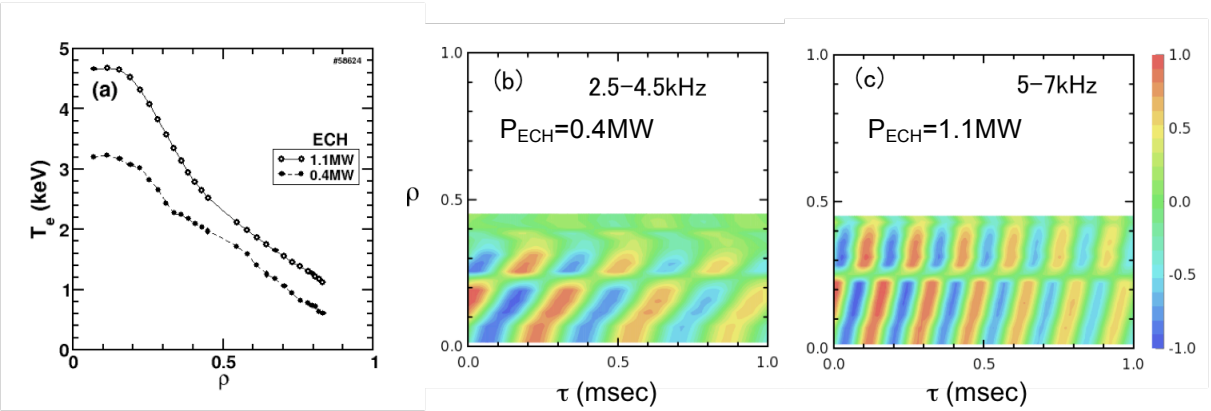

FIG. 4. (a) Typical radial profiles of T_e in the ITB plasmas. Contour plot of the cross-correlation function of the low frequency component (2.5-4.5 kHz (b) and 5-7 kHz (c)) of $\tilde{T}_e$ from 28-ECE channels with that of the reference channel at ρ=0.15(b) and 0.19 (c).

4. Impact of Long-Range Fluctuation at the onset of Improvement of Confinement

Ballistic propagation of the order of 0.1 msec demonstrates that the long-range fluctuation can play a dominant role in transient response. To understand it, the transient transport experiment is useful. A cold pulse is induced in the L-mode LHD plasma using a tracer encapsulated

solid pellet (TESPEL) injection. Then abrupt core T_e rise induced by edge perturbation (TESPEL ablation at $\rho \sim 0.8$) [21] was observed and abrupt reduction of thermal diffusivity was identified just after TESPEL injection. Typical time evolution of T_e in the edge and central region is shown in Fig. 5(a). The T_e in the edge region decreases due to cold electrons provided by TESPEL ablation (TESPEL ablates within 1 msec). While the T_e in the core region begin to increase after 0.1 msec delay. The time evolution of $\tilde{T}_e$ in the frequency band of 1.5-3.5kHz in Figs. 5(b)-(d) shows that the amplitude of fluctuations varies during T_e rise phase. The changes of amplitude of fluctuations, however, have no significant correlation with the onset of T_e rise. Instead, the radial phase relation observed before TESPEL injection, which indicates radial propagation, is changed just after a TESPEL injection in the core region as shown in Figs. 5(e)-(f). In longer time scale, the radial correlation structure is also changed. Figure 6 shows a contour plot of correlations of $\tilde{T}_e$ and a reconstructed image on the poloidal cross-section during T_e rise phase (2.85-2.858 sec). Changes of number of nodes and radial wave number k_r in the core region indicate that wave-front of fluctuation is distorted.

Studies of nonlinear coupling between secondary instabilities with finite k_θ and microscopic fluctuations have been performed [22]. When

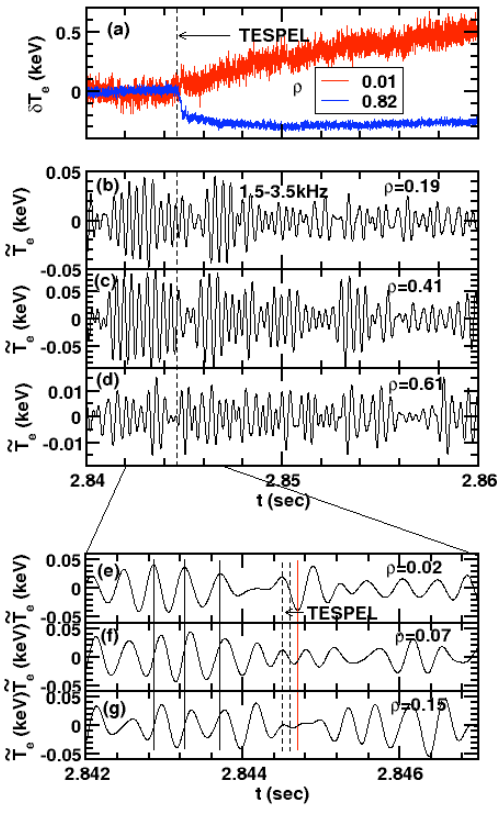

FIG. 5. (a) Time evolution of increment of T_e during nonlocal T_e rise induced by TESPEL injection. Dashed-line indicates the timing of TESPEL injection. (b)-(d)Time evolution of fluctuation in the frequency band of 1.5-3.5 kHz at three different radii.(e)-(g) Change of phase relation of fluctuations in the core region just after TESPEL injection.

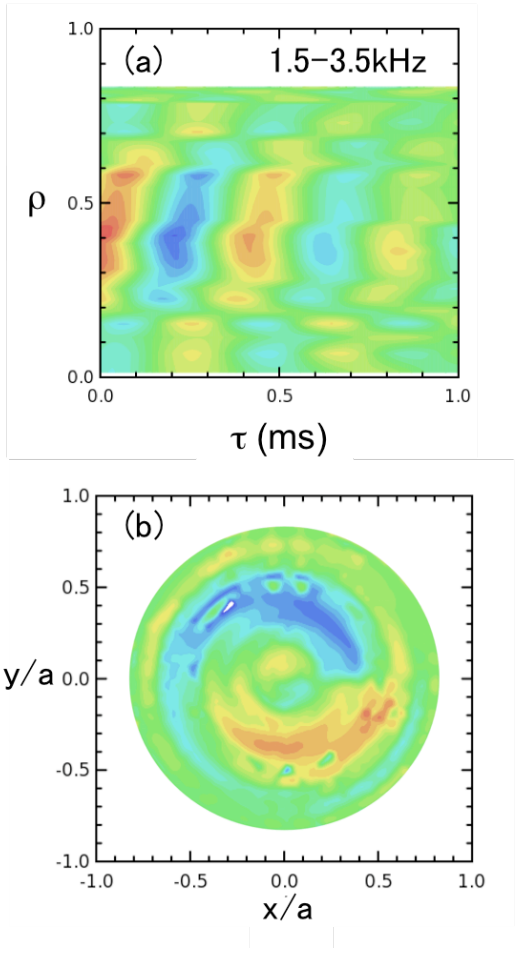

FIG.6. (a) Contour plot of the cross-correlation function of the low frequency component (1.5-3.5 kHz) of $\tilde{T}_e$ during Te rise phase (2.85-2.858 sec) induced by TESPEL injection. (b) Reconstructed image plot of $\tilde{T}_e$ structure on the poloidal cross-section.

microscopic fluctuations excite poloidally symmetric structure nonlinearly with finite k_r, the nonlinear interaction occurs through modulation of k_r rather than that of k_θ. This process is primary mechanism to drive zonal flows by the drift wave [23]. The k_r modulation and the associated nonlinear energy transfer in modulational instability are observed in linear magnetized plasma [24]. The phase dynamics of fluctuation is thus considered to be important to clarify the impacts of long-range fluctuation on transport. There are varieties of reports on the importance of phase dynamics e.g. [25, 26]. Such approach will be the object of future work.

5. Discussions and Summary

The significant T_e fluctuations in a few kHz band are routinely observed in the low collisionality region of LHD plasmas (frequency and amplitude of fluctuation vary depending on discharge). The existence of low frequency temperature fluctuations was also suggested in many toroidal plasmas [27-29]. A strong T_e dependence of fluctuation amplitude (T_e^4) was observed in LHD [16] and thus $\tilde{T}_e$ could be distinguishable from noise when T_e is high enough. Fluctuations with long-distance correlation in tokamaks will be observed in the low collisional region by using of the correlation technique.

Pumping of linearly stable modes and quasi-modes, in the low-n drift wave frequency range, by unstable microscopic fluctuations is a possible excitation mechanism of fluctuation with n=1 mode structure [13]. One of the candidates of this low frequency fluctuation is a linearly stable dissipative trapped-ion mode [30]. The influence of orbit width on observed correlation length is small and is not essential. The orbit width of helically trapped electron is much smaller than radial correlation length of $\tilde{T}_e$.

In conclusion, we have identified the large-scale and low frequency electron temperature fluctuations both in L-mode and ITB plasmas. Experimental results show that (i) the radial correlation length of the fluctuations is comparable to plasma radius, (ii) the fluctuations and the change of amplitude propagate radially at a ballistic speed of 1-5 km/s, which is of the order of the diamagnetic drift velocity and (iii) global distortion of wave-front, which is coincided with excitation of edge perturbation, occur before reduction of transport. One of candidates of the long-range fluctuations is the linearly stable dissipative-trapped ion mode. The fluctuations have substantial impact on turbulent transport and could be a leading player in transient transport response phenomena. Identification of long-range fluctuations and observation of phase dynamics of them provide a fundamental basis to understand the ITB formation mechanisms.

Acknowledgement

We thank Prof. P. H. Diamond, Prof. M. Yagi, Prof. A. Fujisawa, Dr. T. Yamada and Dr. Y. Nagashima and for useful discussion. We are grateful to the technical group in NIFS for their excellent support. This work is partly supported by a grant-in-aid for scientific research of JSPF, Japan (21224014, 19360148) and by the collaboration programs of NIFS (NIFS07KOAP017, NIFS10KOAP023) and of the RIAM of Kyushu University and Asada Science foundation.

References

[1] R. C. Wolf, et. al., Plasma Phys. Control. Fusion **45** (2003) R1

[2] K. Itoh, S.-I. Itoh, and A. Fukuyama, *Transport and Structural Formation in Plasmas* (Institute of Physics Publishing, London, 1999)
[3] S. Inagaki, et al., Nucl. Fusion, **46** (2006) 133; T. Fujita, et. al., Phys. Rev. Lett. **78** (1997) 2377
[4] S. Inagaki, et al., Nucl. Fusion, **50** (2010) 064012
[5] K. Ida, et al., Nucl. Fusion **49** (2009) 015005
[6] J.G. Cordey, et al., Plasma Phys. Control. Fusion **36** (1994) A26
[7] Equipe TFR, Plasma Phys. Control. Fusion **28** (1986) 85
[8] E. D. Fredrickson, et al., Phys. Rev. Lett. **65** (1990) 2869
[9] K. W. Gentle, et al., Phys. Plasmas **2** (1995) 2292
[10] U. Stroth, et al., Plasma Phys. Control. Fusion **38** (1996) 1087
[11] T. Iwasaki, et al., J. Phys. Soc. Japan **68** (1999) 478
[12] K. Itoh and S.-I. Itoh, Plasma Phys. Control. Fusion **44** (2002) A367
[13] S.-I. Itoh and K. Itoh, Plasma Phys. Control. Fusion **43** (2001) 1055
[14] P. H. Diamond and T. S. Hahm, Phys. Plasmas **2** (1995) 3640
[15] X. Garbet and R. Waltz, Phys. Plasmas **5** (1998) 2836
[16] S. Inagaki, et al., submitted to Phys. Rev. Lett. (2010)
[17] K. Kawahata, et al., Rev. Sci. Instrum. **74** (2003) 1449
[18] T. Tokuzawa, et al., Proc. 31st EPS conf., P5-114, London, UK (2004).
[19] S. Sakakibara, et al., Nucl. Fusion, **41** (2001) 1177
[20] T. Shimozuma, et al., Plasma Phys. Control. Fusion **45** (2003) 1183
[21] S. Inagaki, et. al., Plasma Phys. Control. Fusion **52** (2010) 075002
[22] T. Yamada, et. al., Nature Phys. **4** (2008) 721
[23] P. H. Diamond, S.-I. Itoh, K. Itoh and T. S. Hahm, Plasma Phys. Control. Fusion **47** (2005) R35
[24] Y. Nagashima, et. al., Phys. Plasmas **16** (2009) 020706
[25] G. I. Sivashinsky, Ann. Rev. Fluid Mech. **15** (1983) 170; G. I. Sivashinsky and D. M. Michelson, Prog. Theor. Phys. **63** (1980) 2112; Y. Kuramoto and T. Tsuzuki, Prog. Theor. Phys. **54** (1975) 687
[26] Yakhot, Phys. Rev. A **24** (1981) 642
[27] S. Sattler and H. J. Hartfuss, Phys. Rev. Lett. **72** (1994) 653
[28] C. Watts and C. F. Gandy, Phys. Rev. Lett. **75** (1995) 1759
[29] P. A. Politzer, Phys. Rev. Lett. **84** (2000) 1192
[30] B. B. Kadomtsev and O. P. Pogutse, Nucl. Fusion **11** (1971) 67